2017 American Control Conference
Sheraton Seattle Hotel
May 24–26, 2017, Seattle, USA

Low-complexity stochastic modeling of spatially-evolving flows

Wei Ran, Armin Zare, M. J. Philipp Hack, and Mihailo R. Jovanović

Abstract— **Low-complexity approximations of the Navier-Stokes (NS) equations are commonly used for analysis and control of turbulent flows. In particular, stochastically-forced linearized models have been successfully employed to capture structural and statistical features observed in experiments and high-fidelity simulations. In this work, we utilize stochastically-forced linearized NS equations and the parabolized stability equations to study the dynamics of flow fluctuations in transitional boundary layers. The parabolized model can be used to efficiently propagate statistics of stochastic disturbances into statistics of velocity fluctuations. Our study provides insight into the interaction of the slowly-varying base flow with streamwise streaks and Tollmien-Schlichting waves. It also offers a systematic, computationally efficient framework for quantifying the influence of stochastic excitation sources (e.g., free-stream turbulence and surface roughness) on velocity fluctuations in weakly non-parallel flows.**

Index Terms— **Boundary layers, distributed systems, energy amplification, parabolized stability equations, stochastically forced Navier-Stokes equations.**

I. Introduction

The analysis, optimization, and control of dynamical models that are based on the Navier-Stokes (NS) equations is often hindered by their complexity and large number of degrees of freedom. While the existence of coherent structures in wall-bounded shear flows [1] has inspired the development of reduced-order models using data-driven techniques, the important features of such models can be crucially altered by control actuation and sensing. This gives rise to nontrivial challenges for model-based control design [2].

In contrast, linearization of the NS equations around mean-velocity is well-suited for analysis and synthesis using tools of modern robust control. Linearized models subject to stochastic excitation have been employed to replicate structural and statistical features of transitional [3]–[5] and turbulent [6]–[8] wall-bounded shear flows. In these models the nonlinear terms in the NS equations are replaced by stochastic forcing. Most studies have focused on parallel flow configurations in which translational invariance allows for the decoupling of the dynamical equations across streamwise and spanwise wavenumbers. This offers significant computational advantages for analysis, optimization, and control.

Financial support from the National Science Foundation under Award CMMI 1363266 and the Air Force Office of Scientific Research under Award FA9550-16-1-0009 is gratefully acknowledged.

Wei Ran, Armin Zare, and Mihailo R. Jovanović are with the Department of Electrical Engineering, University of Southern California, Los Angeles, CA 90089. M. J. Philipp Hack is with the Center for Turbulence Research, Stanford University, Stanford, CA 94305. E-mails: wran@usc.edu, armin.zare@usc.edu, philipp.hack@stanford.edu, mihailo@usc.edu.

In the flat-plate boundary layer streamwise and normal inhomogeneity leads to the temporal eigenvalue problem for PDEs with two spatial variables. This problem is computationally more difficult to solve than for parallel flows. Previously, tools from sparse linear algebra and iterative schemes have been employed to analyze the spectra of the governing equations and provide insight into the dynamics of transitional flows [9]–[11]. Efforts have also been made to conduct non-modal analysis of spatially-evolving flows including transient growth [10], [12] and resolvent [13] analyses. In spite of these successes many challenges remain.

The Parabolized Stability Equations (PSE) result from the removal of elliptic components from the NS equations. The PSE respect inhomogeneity in the streamwise direction but do not propagate information upstream. This makes them computationally more efficient than conventional flow simulations based on the NS equations [14]. In particular, the resulting set of equations are convenient for marching in the downstream direction [15]–[17]. They are thus routinely used to compute the spatial evolution of instability modes in a wide range of engineering problems [17].

Despite their popularity, parabolized equations have been utilized in a rather narrow context. We revisit the modeling of spatially-evolving boundary layer flow by examining the utility of such models in assessing the receptivity and quantifying the sensitivity to different types of flow disturbances. Our simulation-free approach lays the groundwork for a systematic, computationally efficient framework for quantifying the influence of stochastic excitation sources on velocity fluctuations in weakly non-parallel flows.

The paper is organized as follows. In Section II, we describe stochastically-forced linearization of the NS equations around Blasius boundary layer flow. In Section III, we study the receptivity to stochastic excitations of the velocity fluctuations around locally-parallel and spatially evolving Blasius profiles. In Section IV, we adopt stochastic forcing to model the effect of excitations in the PSE. Finally, we provide concluding thoughts in Section V.

II. Background

In this section, we present the equations that govern the dynamics of flow fluctuations in incompressible flows of Newtonian fluids and characterize the structural constraints that are imposed on the second-order statistics by the linearized dynamics.

In a flat-plate boundary layer, with geometry shown in Fig. 1, the dynamics linearized around the Blasius boundary

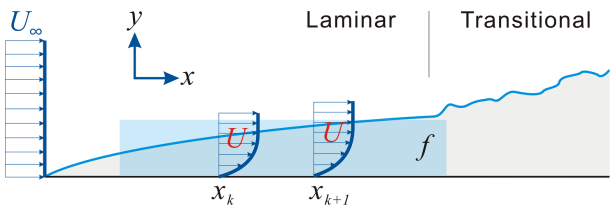

Fig. 1: Geometry of a transitional boundary layer flow subject to stochastic forcing.

layer profile $\bar{\mathbf{u}} = [\,U(x,y)\;\; V(x,y)\;\; 0\,]^T$ are

$$\begin{aligned} \mathbf{v}_t &= -(\nabla\cdot\bar{\mathbf{u}})\,\mathbf{v} - (\nabla\cdot\mathbf{v})\,\bar{\mathbf{u}} - \nabla p + \frac{1}{Re_0}\Delta\mathbf{v} + \mathbf{f}, \\ 0 &= \nabla\cdot\mathbf{v}, \end{aligned} \tag{1}$$

where $\mathbf{v} = [\,v_1\;\; v_2\;\; v_3\,]^T$ is the vector of velocity fluctuations, p denotes pressure fluctuations, and v_1, v_2, and v_3 represent components of the fluctuating velocity field in the streamwise (x), wall-normal (y), and spanwise (z) directions, respectively. The Reynolds number is defined as $Re_0 = U_\infty\delta_0/\nu$, where $\delta_0 = \sqrt{\nu x_0/U_\infty}$ is the Blasius length scale at the inflow, U_∞ is the free-stream velocity, and ν is the kinematic viscosity. Spatial coordinates are non-dimensionalized by δ_0, velocities by U_∞, time by δ_0/U_∞, and pressure by ρU_∞^2, where ρ is the fluid density. The presence of the additive zero-mean stochastic body forcing $\mathbf{f}$ can be justified in different ways [3]–[5]. For our purposes, we wish to compensate the role of the neglected nonlinear interactions by introducing stochastic sources of excitation that perturb the otherwise linearly developing velocity field.

III. Stochastically-forced linearized NS equations

In this section, we first examine the dynamics of flow fluctuations in the stochastically-forced Blasius boundary layer under a locally-parallel base flow assumption. This assumption entails linearization around the Blasius profile evaluated at a fixed streamwise location x_0. Since the resulting base flow only depends on the wall-normal coordinate y, this also allows for the parameterization of the corresponding evolution model over horizontal wavenumbers. This reduces the computational complexity of studying the amplification of streamwise streaks and Tollmien-Schlichting (TS) waves, which are of importance in the laminar-turbulent transition of boundary layer flows. We then repeat the same exercise for the NS equations linearized around a base flow profile which is a function of both streamwise and wall-normal coordinates. In fluids literature this approach is called *global analysis* and it is typically computationally challenging. We have ensured grid convergence by doubling the number of points used to discretize the differential operators in the streamwise and wall-normal coordinates.

A. Parallel Blasius boundary layer flow subject to free-stream turbulence

We perform an input-output analysis to quantify the energy amplification of velocity fluctuations subject to an exogenous source of excitation that represents free-stream turbulence. This excitation is modeled as white-in-time stochastic forcing into the linearized NS equations around the parallel Blasius base flow profile, i.e., the Blasius profile evaluated at one streamwise location x_0. This choice is motivated by previous studies which show that transient growth exhibits similar trends for parallel and non-parallel boundary layer flows [18], [19].

Under the assumption of a parallel base flow, translational invariance allows us to apply Fourier transform in the plate-parallel directions. This brings the state-space representation of the linearized NS equations to the form

$$\begin{aligned} \dot{\boldsymbol{\psi}}(\mathbf{k},t) &= A(\mathbf{k})\,\boldsymbol{\psi}(\mathbf{k},t) + B(\mathbf{k})\,\mathbf{f}(\mathbf{k},t), \\ \mathbf{v}(\mathbf{k},t) &= C(\mathbf{k})\,\boldsymbol{\psi}(\mathbf{k},t). \end{aligned} \tag{2}$$

Here, $\boldsymbol{\psi} = [\,v_2^T\;\; \eta^T\,]^T \in \mathbb{C}^{2N_y}$ is the state, which contains the wall-normal velocity v_2 and vorticity η , and $\mathbf{v} \in \mathbb{C}^{3N_y}$ with N_y being the number of collocation points in the finite dimensional approximation of the differential operators in the wall-normal direction. Equations (2) are parameterized by the spatial wavenumber pair $\mathbf{k} = (k_x, k_z)$; see [5] for the expressions of A, B, and C. We consider no-slip and no-penetration boundary conditions.

In statistical steady-state, the covariance matrix

$$\Phi(\mathbf{k}) = \lim_{t\to\infty} \mathbf{E}\left(\mathbf{v}(\mathbf{k},t)\,\mathbf{v}^*(\mathbf{k},t)\right)$$

of the velocity fluctuation vector, and the covariance matrix

$$X(\mathbf{k}) = \lim_{t\to\infty} \mathbf{E}\left(\boldsymbol{\psi}(\mathbf{k},t)\,\boldsymbol{\psi}^*(\mathbf{k},t)\right),$$

of the state in (2), are related as follows:

$$\Phi = C\,X\,C^*.$$

Here, $*$ denotes complex-conjugate-transpose and $\mathbf{E}$ is the expectation operator. Matrix Φ contains information about all second-order statistics of the fluctuating velocity field.

For a stable dynamical generator A, the steady-state covariance of the state in (2) subject to zero-mean and white-in-time stochastic forcing with covariance $\Omega = \Omega^* \succeq 0$, i.e.,

$$\mathbf{E}\left(\mathbf{f}(t_1)\,\mathbf{f}^*(t_2)\right) = \Omega\,\delta(t_1 - t_2),$$

is determined by the solution to the Lyapunov equation,

$$A\,X + X\,A^* = -B\,\Omega B^*. \tag{3}$$

The energy amplification of the stochastically-forced flow can be computed using the solution to the Lyapunov equation (3) as:

$$E = \operatorname{trace}\left(C\,X\,C^*\right). \tag{4}$$

The receptivity to external forcing that enters in various wall-normal locations can be evaluated by computing the energy spectrum of the velocity fluctuations. To specify the wall-normal region in which the forcing enters, we define

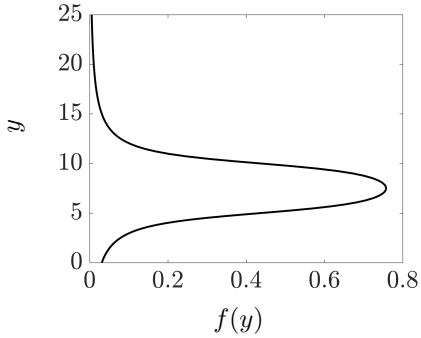

Fig. 2: The shape of the filter function $f(y)$; $y_1 = 5$, $y_2 = 10$.

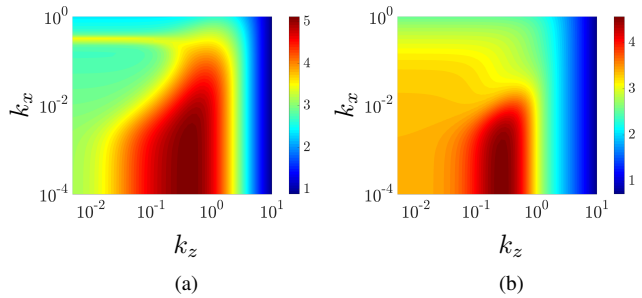

Fig. 3: Plots of $\log_{10}(E(\mathbf{k}))$ in the Blasius boundary layer flow with $Re_0 = 400$ subject to white-in-time stochastic excitation entering in various wall-normal regions; (a) $y_1 = 0$, $y_2 = 5$ (b) $y_1 = 5$, $y_2 = 10$ in Eq. (5).

$\mathbf{f} := f(y)\mathbf{f}_s$ where $\mathbf{f}_s$ represents the solenoidal forcing arising from free-stream turbulence and $f(y)$ is the smooth filter function defined as

$$f(y) := \frac{1}{\pi}\left(\text{atan}(y - y_1) - \text{atan}(y - y_2)\right). \quad (5)$$

Here, y_1 and y_2 determine the shape of $f(y)$; Fig. 2 shows $f(y)$ when $y_1 = 5$ and $y_2 = 10$.

We compute the energy spectrum of stochastically excited parallel Blasius boundary layer flow with $Re_0 = 400$ (the Blasius length scale is $\delta_0 = 1$). Here, we consider a wall-normal region with $L_y = 25$. A solenoidal white-in-time excitation $\mathbf{f}_s$ is first introduced to the region in the immediate vicinity of the wall by choosing $y_1 = 0$ and $y_2 = 5$ in Eq. (5). Figure 3a shows that the energy of velocity fluctuations is most amplified at low streamwise wavenumbers ($k_x \approx 0$) with a global peak at $k_z \approx 0.42$. Clearly, the energy spectrum is dominated by streamwise elongated flow structures, with TS waves observed at $k_x \approx 0.35$. As the forcing region moves away from the wall the amplification of streamwise elongated structures persists while the amplification of the TS waves weakens; see Fig. 3b. It is also observed that as the region of excitation moves away from the wall, energy amplification becomes weaker and the peak of the energy spectrum shifts to lower values of k_z. These observations are in agreement with the global analysis of boundary layer flow presented next.

B. Global analysis of stochastically-forced linearized NS equations

We consider the linearized NS equations around a spatially-evolving Blasius boundary layer profile and introduce forcing at various wall-normal locations. To capture the spatially evolving nature of the boundary layer, we employ finite dimensional spatial discretization in both streamwise and wall-normal directions. The linearized NS generator is globally stable for the particular Reynolds number and spanwise wavenumbers we consider in this study. Thus, the steady-state covariance of the fluctuating velocity field can be obtained from the solution to the Lyapunov equation (3).

The computational region is a rectangular box with $L_x \times L_y = 900 \times 25$ and the initial Reynolds number is $Re_0 = 400$. We consider the linearized dynamics given in Eqs. (2) with state $\boldsymbol{\psi} = [\, v_2^T \;\; \eta^T \,]^T \in \mathbb{C}^{2N_xN_y}$, $\mathbf{k} = k_z$, and differential operators that are now spatially discretized in both wall-normal and streamwise directions. Here, N_x and N_y denote the number of collocation points in the streamwise and wall-normal directions, respectively. We enforce homogenous Dirichlet boundary conditions on η and Dirichlet/Neumann boundary conditions on v_2 and introduce Sponge layers in the streamwise direction to mitigate the influence of boundary conditions on the fluctuation dynamics [20], [21]. Similar to Section III-A, we assume that white-in-time stochastic forcing is filtered by the function $f(y)$ in (5).

Our computational experiments show that the energy amplification increases as the region of influence for the external forcing approaches the wall; for $k_z = 0.4$, the energy amplification (cf. Eq. (4)) for perturbations that enter in the vicinity of the wall ($y_1 = 0$ and $y_2 = 5$ in Eq. (5)) and away from the wall ($y_1 = 5$ and $y_2 = 10$) is 3.9×10^6 and 4.0×10^5, respectively. Figures 4a and 4b show the spatial structure of the streamwise component of the principal response when white-in-time stochastic forcing enters in the vicinity of the wall and away from the wall, respectively. The streamwise growth of the streaks can be observed. Figures 4c and 4d display the cross-section of these streamwise elongated structures at $z = 0$. As Figs. 4e and 4f demonstrate, these streaky structures are sandwiched between counter-rotating vortical motions in the cross-stream plane; and they contain alternating regions of fast- and slow-moving fluid that are slightly inclined to the wall.

IV. Stochastically-forced linear parabolized stability equations

While it is customary to use the parallel-flow approximation to study the stability of boundary layer flows to small amplitude perturbations, this approximation does not accurately capture the effect of the spatially-evolving base flow on the stability of the boundary layer. This issue can

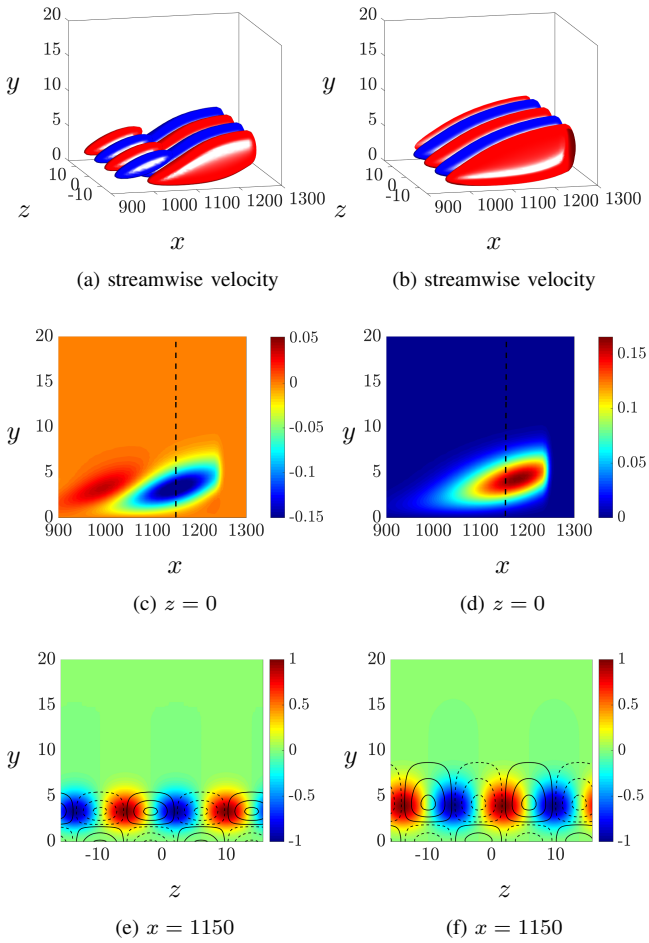

Fig. 4: Principal modes with $k_z = 0.4$, resulting from exitation in the vicinity (a,c,e) ($y_1 = 0$ and $y_2 = 5$ in (5)) and away from the wall (b,d,f) ($y_1 = 5$ and $y_2 = 10$ in (5)). (a,b) Streamwise velocity component where red and blue colors denote regions of high and low velocity; (c,d) streamwise velocity at $z = 0$; (e,f) y-z slice of streamwise velocity (color plots) and vorticity (contour lines) at $x = 1150$.

be addressed by examining the spatial growth of specific wave structures. Furthermore, in the absence of body forcing and neutrally stable modes, linearized models that do not account for the spatial evolution of the base flow predict either asymptotic decay or unbounded growth of fluctuations. On the other hand, the global analysis and direct numerical simulation of spatially-evolving flows may be prohibitively expensive for analysis and control purposes.

To refine predictions of parallel flow analysis, we utilize the Parabolized Stability Equations (PSE) to study the dynamics of flow fluctuations in flat-plate boundary layers. These equations are obtained by removing elliptic components from the NS equations and they can be easily advanced downstream via a marching procedure. This approach is significantly more efficient than conventional flow simulations based on the NS equations. In contrast to standard PSE-based analysis, we introduce a stochastic forcing term and show that linear PSE can be used to march covariance matrices downstream in a computationally efficient manner.

We next provide a brief overview of the stochastically-forced linear PSE. Additional details regarding the PSE can be found in [15], [16].

A. Linear parabolized stability equations

In weakly non-parallel flows, e.g. the pre-transitional boundary layer, flow fluctuations can be separated into slowly and rapidly varying components [15]. This is achieved by considering the following decomposition for the fluctuation field $\hat{\mathbf{q}} = [\, v_1 \;\; v_2 \;\; v_3 \;\; p \,]^T$ in (1),

$$\hat{\mathbf{q}}(x,y,z,t) \;=\; \mathbf{q}(x,y)\,\chi(x,z,t) \;+\; \text{complex conj.},$$

$$\chi(x,z,t) \;=\; \exp\left(\mathrm{i}\left(\theta(x) \;+\; k_z\, z \;-\; \omega\, t\right)\right),$$

$$\theta(x) \;=\; \int_{x_0}^{x} \alpha(\xi)\,\mathrm{d}\xi,$$

where $\mathbf{q}(x,y)$ and $\chi(x,z,t)$ are the shape and phase functions, k_z and ω are the spanwise wavenumber and temporal frequency, and $\alpha(x)$ is the streamwise varying generalization of the wavenumber [15]. The ambiguity arising from the streamwise variation of both $\mathbf{q}$ and α is resolved by imposing the condition $\int_{\Omega_y} \mathbf{q}^*\mathbf{q}_x \,\mathrm{d}y = 0$ [15]. The PSE approximation assumes the streamwise variation of $\mathbf{q}$ and α as sufficiently small to neglect $\mathbf{q}_{xx}$, α_{xx}, $\alpha_x\mathbf{q}_x$, and their higher order derivates with respect to x. The stochastically-forced linear PSE thus take the form

$$L\,\mathbf{q} \;+\; M\,\mathbf{q}_x \;+\; \alpha_x\, N\,\mathbf{q} \;=\; \mathbf{f}, \tag{6}$$

where expressions for operator-valued matrices L, M, and N can be found in [16]. We discretize these operators using a pseudospectral scheme with N_y Chebyshev collocation points in the wall-normal direction [22].

In what follows, we use the PSE to propagate the spatially-evolving state covariance,

$$X(x) \;=\; \mathbf{E}\left(\mathbf{q}(x)\,\mathbf{q}^*(x)\right),$$

via the Lyapunov equation

$$X_{k+1} \;=\; \bar{A}_{k+1}\, X_k\, \bar{A}^*_{k+1} \;+\; \bar{B}\,\Omega_{k+1}\bar{B}^*, \tag{7}$$

where $\mathbf{E}$ is the expectation operator, k identifies the streamwise location, and Ω_k represents the covariance of the white stochastic disturbance $\mathbf{f}$. The dynamical matrix $\bar{A}$ and the input matrix $\bar{B}$ result from a rearrangement of the stochastically-forced linear PSE (6) with a constant streamwise wavenumber α,

$$\mathbf{q}_x \;=\; \underbrace{(-M^{-1}L)}_{\bar{A}}\,\mathbf{q} \;+\; \underbrace{(-M^{-1})}_{\bar{B}}\,\mathbf{f}.$$

These equations provide a good approximation of perturbations with slowly-varying streamwise wavenumbers [23]. The streamwise dependence of our equations follows from the dependence of the state $\mathbf{q}$, and matrices L and M on the streamwise location x_k. Propagation of the state covariance X_k using Eq. (7) offers significant computational advantage

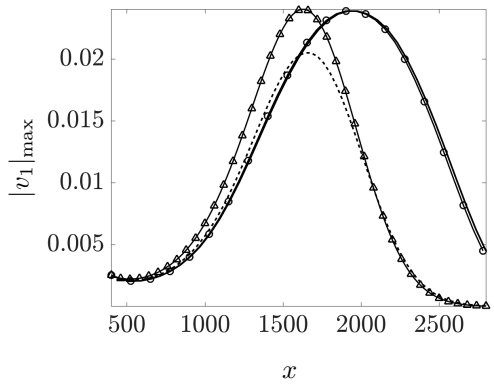

Fig. 5: Peak of the amplitude of TS waves at $\omega = 0.0344$ in a flat-plate boundary layer flow; nonlinear PSE (solid), linear PSE without forcing (dashed), linear PSE with white forcing ($\triangle$), and linear PSE with white, but x-dependent forcing designed using the procedure explained in Section IV-B ($\bigcirc$).

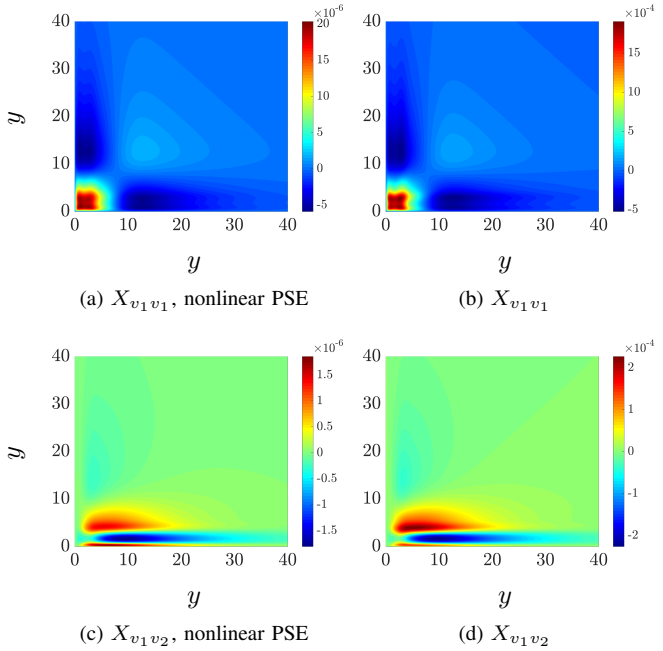

Fig. 6: Velocity covariance matrices at $x = 2800$ resulting from (a,c) simulation of nonlinear PSE, and (b,d) from propagation of Eq. (7) in Blasius boundary layer flow with TS mode initialization. (a,b) The streamwise correlation matrix $X_{v_1v_1}$, and (c,d) the streamwise/wall-normal cross correlation matrix $X_{v_1v_2}$.

over computation of the covariance from the ensemble average of many stochastic simulations.

We next consider the streamwise evolution of a two-dimensional TS wave and provide a comparison of the results obtained using linear PSE with and without stochastic forcing and nonlinear PSE. In this context, the results of nonlinear PSE, which we consider as the ground-truth, closely match the results of direct numerical simulations [15].

B. Streamwise evolution of a two-dimensional TS wave

We study the streamwise evolution of a two-dimensional TS wave ($k_z = 0$) with an initial amplitude of 2.5×10^{-3} and temporal frequency $\omega = 0.0344$. All computations are initialized at $Re_0 = 400$ with the streamwise wavenumber α and shape function corresponding to the considered TS-mode. This mode is identified by the eigenvalue with the largest imaginary part in the spatial eigenvalue problem. This problem studies the stability of the linearized NS equations for a particular Reynolds number, spanwise wavenumber, and temporal frequency.

The computational domain is $L_x \times L_y = 2400 \times 60$ with homogenous Dirichlet boundary conditions applied in the wall-normal direction. We conduct 400 simulations of stochastically-forced linear PSE (6), with different realizations of white stochastic forcing. As in Section III-A, we filter the forcing using the function $f(y)$ in (5) with $y_1 = 0$ and $y_2 = 10$. The velocity profiles and covariances that result from the ensemble average of these simulations are compared with the results of linear and nonlinear PSE with no stochastic forcing under the same parameter space and initial conditions.

Figure 5 shows the peak amplitude of the streamwise velocity component of the TS wave. Relative to nonlinear PSE, linear PSE with and without white stochastic forcing underestimates the streamwise location of the peak. Figure 6 shows covariance matrices of the streamwise and streamwise/wall-normal velocity components at the outflow ($x = 2800$). These are obtained using simulations of nonlinear PSE and propagation of Eq. (7). We see that the outflow velocity covariances resulting from linear PSE with white forcing capture the essential trends observed in nonlinear PSE.

Our computations show that it is not feasible to exactly match velocity correlations and growth trends with an x-independent white stochastic excitation of the linear PSE. This necessitates the use of x-dependent or colored forcing. As we show next, a forcing field which is streamwise dependent but uncorrelated in the wall-normal direction enables us to better predict the location of the peak amplitude in Fig. 5.

In order to obtain this forcing, we first use X_k and X_{k+1} resulting from nonlinear PSE to compute the covariance $Z_k := \bar{B}\,\Omega_k \bar{B}^*$. This covariance corresponds to a spatially correlated process in the streamwise direction and is thus x-dependent and not necessarily positive semi-definite. We then project these forcing correlations onto the positive-definite cone to obtain uncorrelated noise in the wall-normal direction. The result of incorporating this white but x-dependent forcing is also shown in Fig. 5. Clearly, the peak amplitude resulting from this model matches the curve from nonlinear PSE simulations.

To further evaluate the performance of this model, we examine the error in matching the full state covariance matrix

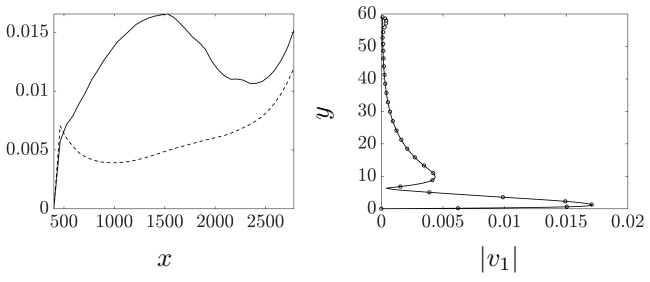

(a) (b)

Fig. 7: (a) Relative error in matching the amplitude of streamwise velocity (solid) and in matching the state covariance $X(x)$ (dashed) using the linear PSE with x-dependent white forcing in the spatial evolution of a 2D TS wave with $\omega = 0.0344$. (b) The amplitude of the streamwise component of a 2D TS waves at $x = 1528$ from nonlinear PSE (solid) and stochastically forced linear PSE ($\bigcirc$).

X and the amplitude of the streamwise velocity profile $|v_1|$ as a function of the streamwise location x; see Fig. 7a. This figure shows that the streamwise velocity amplitude and covariance matrices are reasonably recovered. Figure 7b shows the amplitude of the streamwise velocity $|v_1|$ at the location with highest error ($x = 1528$). The profiles resulting from linear PSE with x-dependent white forcing perfectly match the results of nonlinear PSE.

V. Concluding remarks

In the present study, we have utilized stochastically-forced linearized NS equations and stochastically-forced linear PSE to study the dynamics of flow fluctuations in the Blasius boundary layer. In particular, we have examined the receptivity of the spatially-evolving Blasius boundary layer flow to free-stream disturbances which we model as stochastic excitations that enter at specific wall-normal locations. We also incorporate stochastic forcing into the linear PSE to study the streamwise evolution of TS waves. While white stochastic excitation is not able to improve predictions relative to the conventional linear PSE without stochastic forcing, we achieve better predictions of transient peaks using white, but x-dependent forcing. The predictive power of our approach can be further improved by utilizing recently developed theoretical framework for identifying the spatio-temporal spectrum of stochastic excitation sources [8], [24]. The problem of employing such a framework in order to recover partially-observed statistical signatures of spatially-evolving flows via low-complexity stochastic models will be studied in our future work.

References

[1] A. J. Smits, B. J. McKeon, and I. Marusic, "High-Reynolds number wall turbulence," *Ann. Rev. Fluid Mech.*, vol. 43, pp. 353–375, 2011.

[2] B. R. Noack, M. Morzyński, and G. Tadmor, *Reduced-order modelling for flow control*, ser. CISM Courses and Lectures. Springer, 2011, vol. 528.

[3] B. F. Farrell and P. J. Ioannou, "Stochastic forcing of the linearized Navier-Stokes equations," *Phys. Fluids A*, vol. 5, no. 11, pp. 2600–2609, 1993.

[4] B. Bamieh and M. Dahleh, "Energy amplification in channel flows with stochastic excitation," *Phys. Fluids*, vol. 13, no. 11, pp. 3258–3269, 2001.

[5] M. R. Jovanović and B. Bamieh, "Componentwise energy amplification in channel flows," *J. Fluid Mech.*, vol. 534, pp. 145–183, July 2005.

[6] Y. Hwang and C. Cossu, "Linear non-normal energy amplification of harmonic and stochastic forcing in the turbulent channel flow," *J. Fluid Mech.*, vol. 664, pp. 51–73, 2010.

[7] R. Moarref and M. R. Jovanović, "Model-based design of transverse wall oscillations for turbulent drag reduction," *J. Fluid Mech.*, vol. 707, pp. 205–240, September 2012.

[8] A. Zare, M. R. Jovanović, and T. T. Georgiou, "Colour of turbulence," *J. Fluid Mech.*, vol. 812, pp. 636–680, February 2017.

[9] U. Ehrenstein and F. Gallaire, "On two-dimensional temporal modes in spatially evolving open flows: the flat-plate boundary layer," *J. Fluid Mech.*, vol. 536, pp. 209–218, 2005.

[10] E. Åkervik, U. Ehrenstein, F. Gallaire, and D. S. Henningson, "Global two-dimensional stability measures of the flat plate boundary-layer flow," *Eur. J. Mech. B*, vol. 27, no. 5, pp. 501–513, 2008.

[11] G. P. Paredes, "Advances in global instability computations: from incompressible to hypersonic flow," Ph.D. dissertation, Technical University of Madrid, 2014.

[12] A. Monokrousos, E. Åkervik, L. Brandt, and D. S. Henningson, "Global three-dimensional optimal disturbances in the blasius boundary-layer flow using time-steppers," *J. Fluid Mech.*, vol. 650, pp. 181–214, 2010.

[13] J. Jeun, J. W. Nichols, and M. R. Jovanović, "Input-output analysis of high-speed axisymmetric isothermal jet noise," *Phys. Fluids*, vol. 28, no. 4, p. 047101 (20 pages), April 2016.

[14] M. J. P. Hack and P. Moin, "Towards modeling boundary layer transition in large-eddy simulations," in *Annual Research Briefs*, Center for Turbulence Research, Stanford University, 2015, pp. 137–144.

[15] F. P. Bertolotti, T. Herbert, and P. R. Spalart, "Linear and nonlinear stability of the Blasius boundary layer," *J. Fluid Mech.*, vol. 242, pp. 441–474, 1992.

[16] T. Herbert, "Parabolized stability equations," in *Special Course on Progress in Transition Modelling*. AGARD Rep., 1994, ch. 4, pp. 1–34, No. 793.

[17] T. Herbert, "Parabolized stability equations," *Annu. Rev. Fluid Mech.*, vol. 29, no. 1, pp. 245–283, 1997.

[18] P. Andersson, M. Berggren, and D. Henningson, "Optimal disturbances and bypass transition in boundary layers," *Phys. Fluids*, vol. 11, no. 1, pp. 134–150, 1999.

[19] A. Tumin and E. Reshotko, "Spatial theory of optimal disturbances in boundary layers," *Phys. Fluids*, vol. 13, pp. 2097–2104, 2001.

[20] J. W. Nichols and S. K. Lele, "Global modes and transient response of a cold supersonic jet," *J. Fluid Mech.*, vol. 669, pp. 225–241, 2011.

[21] A. Mani, "Analysis and optimization of numerical sponge layers as a nonreflective boundary treatment," *J. Comput. Phys.*, vol. 231, no. 2, pp. 704–716, 2012.

[22] J. A. C. Weideman and S. C. Reddy, "A MATLAB differentiation matrix suite," *ACM Trans. Math. Software*, vol. 26, no. 4, pp. 465–519, December 2000.

[23] A. Towne, "Advancements in jet turbulence and noise modeling: accurate one-way solutions and empirical evaluation of the nonlinear forcing of wavepackets," Ph.D. dissertation, California Institute of Technology, 2016.

[24] A. Zare, Y. Chen, M. R. Jovanović, and T. T. Georgiou, "Low-complexity modeling of partially available second-order statistics: theory and an efficient matrix completion algorithm," *IEEE Trans. Automat. Control*, 2016, doi:10.1109/TAC.2016.2595761.